SWELLING BEHAVIOR OF Na- AND Ca-MONTMORILLONITE UP TO 150ºC BY *IN SITU* X-RAY DIFFRACTION EXPERIMENTS

SHOJI MORODOME AND KATSUYUKI KAWAMURA*

Department of Earth and Planetary Science, Tokyo Institute of Technology, Ookayama 2-12-1-I2, Meguro-ku, Tokyo 152-8551, Japan

Abstract—The effects of temperature on the swelling properties of smectites are important for a variety of different geological conditions, but studies on this topic have been rather limited. The purpose of this study was to investigate the swelling behavior of Na- and Ca-montmorillonite at various temperatures greater than room temperature, up to 150ºC, using *in situ* X-ray diffraction (XRD) analysis. A sample chamber was designed, the temperature and humidity of which were controlled precisely, for environmental *in situ* measurements. The XRD measurements were performed at small relative humidity (RH) intervals for precise observation of the swelling behavior.

The swelling behavior of Na-montmorillonite showed distinct zero-, one-, and two-layer hydration states. The basal spacings of Na-montmorillonite changed continuously with RH for various temperatures in the transition region between the zero- and one-layer hydration states, and the swelling curves of the transition region moved to greater degrees of RH with increasing temperature. The basal spacings jumped from the one- to two-layer hydration states for all temperatures at almost the same RH.

The basal spacings of Ca-montmorillonite changed continuously from the zero- to the two-layer hydration states at all temperatures. This behavior is remarkably different from that of Na-montmorillonite. At low-RH conditions, the d_{001} value of Ca-montmorillonite decreased with increasing temperature. The swelling curves of Ca-montmorillonite did not show a plateau at any temperature for the one-layer hydration state. The swelling curves of Ca-montmorillonite moved to greater RH with temperature, similar to the transformation region between the zero- and one-layer hydration states in Na-montmorillonite. These differences between Na- and Ca-montmorillonite are related to the hydration powers of exchangeable cations.

Key Words—Basal Spacing, Hydration, Interlayer Cation, Montmorillonite, Relative Humidity, Smectite, Swelling, Vapor Pressure, X-ray Diffraction.

INTRODUCTION

The expandability of smectites is a remarkable property, and has been studied by many researchers. Nagelschmidt *et al*. (1936) and Bradley *et al*. (1937), using XRD measurements, demonstrated the incremental increase in basal spacing with water content. Hendricks *et al*. (1940) and Mooney *et al*. (1952) suggested the layer concept, *i.e.* that zero-, one-, two-, and three-water molecular layer hydration states exist in the smectite interlayer. Mooney *et al*. (1952), using XRD, observed the swelling behavior of various homo-ionic montmorillonites *vs*. RH, and showed that the swelling behavior was affected by the kind and valence of the exchangeable cations. Suquet *et al.* (1975) estimated, by means of XRD, the influence of each of surface charge density, charge location, and exchangeable cation on the swelling properties for saponites, montmorillonites, beidellites, and vermiculites and stated that the total layer charge plays a major role in the expansion properties of layer silicates.

Using *in situ* XRD, Watanabe and Sato (1988) observed the swelling behavior of homo-ionic montmorillonites and saponites (Na$^+$, K$^+$, and Ca^{2+}). The swelling behavior of Na- and Ca-montmorillonite differed significantly over the RH range of 0 to 60%. At 60% RH for Na-montmorillonite, an irrational 001 reflection was observed. Watanabe and Sato (1988) suggested that a segregation structure had been formed, and that the existence of two phases indicates heterogeneity in layer charge density. By means of *in situ* XRD, Sato *et al*. (1992) observed the swelling behavior of ten homo-ionic smectites which differed in terms of the amount and location of the layer charge. They suggested that the swelling behavior of smectites is due to the combined effects of the location and amount of charge. Also using *in situ* XRD, Prost (1975) observed systematically the swelling behavior of eight homo-ionic hectorites. The hectorites with Na$^+$, Li$^+$, K$^+$, Ca^{2+}, Mg^{2+}, Sr^{2+}, and Ba^{2+} ions swelled to the zero-, one-, and two-layer hydration states with increasing water content. Cs-hectorite, however, swelled to only the one-layer hydration state. Nakazawa *et al*. (1992) synthesized large crystals of smectite, with a composition similar to that of Na-montmorillonite, by quenching a hydrothermal product at very high pressures and temperatures (*e.g.* 5.5 GPa and 1600ºC). The dimensions of the smectite were

~10 μm or more. Using the *in situ* XRD technique, Yamada *et al*. (1994) examined the swelling behavior of this synthetic smectite. The basal spacing increased in distinctly stepwise fashion with increasing RH. The full-width at half-maximum (FWHM) of the 001 reflection was extremely small compared with that of naturally occurring smectites. Using *in situ* XRD, Tamura *et al*. (2000) observed the swelling behavior of the synthetic smectites with various exchangeable cations, including Na^+, Li^+, K^+, Ca^{2+}, and Mg^{2+}. These smectites showed distinct stepwise hydration *vs*. RH. They stated that the large FWHM of the 001 reflections and the continuous hydration in natural smectite relate to the randomness in layer stacking which is probably caused by a heterogeneous charge distribution in the 2:1 layers and small particle size. Ferrage *et al*. (2005a) examined systematically the swelling behavior of homo-ionic, low-charge montmorillonites (Li^+, Na^+, K^+, Mg^{2+}, Ca^{2+}, and Sr^{2+}) and Ferrage *et al*. (2007) did the same for homoionic, low- and high-charge montmorillonites and beidellites.

In all the studies above, the swelling behavior was analyzed at RH intervals of ~10%. The swelling behavior is difficult to understand in detail, especially during the transition between two hydration states, because the basal spacing may have changed significantly over a very small RH interval. The *in situ* XRD measurements need to be performed over smaller RH intervals for better understanding of the swelling behavior, and to achieve this, precise control of the humidity and temperature is required. In addition, the swelling properties were measured only at room temperature in the aforementioned studies. Observation of swelling behavior over a range of temperatures may improve our understanding of it. Understanding swelling behavior at high temperatures is also important for engineering applications of clays and for disposal of high-level radioactive waste.

Simulations of XRD patterns for one-dimensionally disordered crystals were performed using model structures (Kakinoki and Komura, 1954; MacEwan, 1958; Reynolds and Hower, 1970; Watanabe, 1988), and this idea has been applied to the analysis of swelling behavior (Ben Brahim *et al*., 1983; Moore and Hower, 1986; Iwasaki and Watanabe, 1988). Ferrage *et al*. (2005a, 2005b, 2007) performed XRD profile modeling of 00*l* reflections to analyze the swelling behavior. They obtained good fits for the experimental patterns by their model and discussed the homogeneity or heterogeneity of smectite hydration, the change in the interlayer distances, the coherent scattering domain size, and the distribution of interlayer water *vs*. RH, exchangeable cations, and the amount and location of the layer charge.

The purpose of the present study was to investigate, using *in situ* XRD measurements, the swelling properties of Na- and Ca-montmorillonites at various temperatures greater than room temperature up to 150ºC, and to investigate the differences between the swelling behavior of Na- and Ca-montmorillonites at various temperatures. Na^+ and Ca^{2+} as exchangeable cations of smectite are common in nature and in industrial applications. These two cations have similar ionic radii and are representative monovalent and divalent cations at the Earth's surface. For the collection of XRD profiles, a sample chamber was designed in which the temperature and humidity were controlled precisely and independently.

Clays with mainly Na^+ or Ca^{2+} exchangeable cations are candidate materials for engineered barriers for disposal of high-level radioactive waste. The engineered barrier material is envisaged to come into contact with a canister which contains radioactive waste, and the temperature may be as much as ~100ºC. Keeping the swelling properties stable at these elevated temperatures is important. The engineered barrier may also have contact with concrete walls that include Ca^{2+} cations. In such conditions, the Na^+ cation of the clay mineral may be exchanged by the Ca^{2+} cation. Prediction of the long-term behavior of the engineered barrier must take into account the effect of cation exchange on the swelling properties.

EXPERIMENTAL

Sample preparation

The material used in this study was montmorillonite (Kunipia-F, Kunimine Industry Co. Ltd., Japan), which is from the Tukinuno Mine, Yamagata prefecture, Japan, and is the smectite-enriched fraction of a bentonite rock. Kunipia-F is produced by crushing the bentonite, purifying it by hydraulic elutriation, and drying it at 140ºC (H. Ito, Kunimine Industry Co. Ltd., pers. comm.). The chemical formula of the montmorillonite was reported as $Na_{0.42}Ca_{0.068}K_{0.008}(Al_{1.56}Mg_{0.31}Fe(III)_{0.09}Fe(II)_{0.01})(OH)_2(Si_{3.91}Al_{0.09})O_{10}$ (Ito *et al*., 1993). The layer-charge density of this high-charge montmorillonite is calculated as 0.564 charges per formula unit. Ion-exchange experiments, using 1 mol/L aqueous solutions of NaCl (300 mL) and 0.5 mol/L of $CaCl_2$ (300 mL), were performed with montmorillonite (3 g) in order to obtain monocationic Na- or Ca-montmorillonite, respectively. The solutions were agitated by a stirrer for 30 min. The montmorillonite was separated from the suspension by centrifugation for 12 min at 4000 rpm. This process was repeated three times. Using the same process, the montmorillonite was washed with pure water three times. Finally, the montmorillonite was dried in an oven at 100ºC. To confirm that these processes had no effect on the swelling property, Na-exchanged montmorillonite from the original bentonite of Tukinuno Mine was also prepared. The original bentonite was crushed and purified by hydraulic elutriation, and the ion-exchange experiment was performed using the purified sample in order to obtain the monocationic Na-type sample. The

sample was dried at 40ºC. These processes were all carried out at 40ºC or less. No significant difference in swelling behavior between the sample and Na-exchanged montmorillonite dried at 100ºC was confirmed. The cation contents were checked semi-quantitatively by scanning electron microscopy and energy dispersive spectroscopy (SEM-EDS). The montmorillonite sample was mixed with water in an agate mortar, painted onto a ceramic tile (10 mm × 20 mm), and dried at room temperature for XRD measurements. Montmorillonite samples with exchangeable cations of Na and Ca are denoted hereafter as Na-montmorillonite and Ca-montmorillonite, respectively.

Environmental sample chamber for XRD measurements

A modified version of the sample chamber suggested by Kawamura *et al.* (1999), in which temperature and humidity were controlled precisely and independently (Figure 1), was used. The temperature of the sample was controlled from 40 to 150ºC by circulating silicone oil through the sample chamber using an oil bath. The temperature of the vapor generator was varied from 6 to 94ºC, with water circulated using a water bath. Air was blown into pure water from a micro filter by an air pump. H_2O-saturated vapor from $P(H_2O) = 0.93$ kPa (the vapor generator temperature = 6ºC) up to 81.47 kPa (94ºC) was generated and introduced into the sample chamber. This device prevents the sample from reaching a saturated condition at sample temperatures >100ºC. The RH in the sample chamber was calculated from the sample temperature and the $P(H_2O)$ at vapor-generator temperature. Both the oil and water baths were controllable to a precision of ±0.1ºC. The sample and vapor-generator temperatures were monitored using a digital thermometer with chromel-alumel thermocouples. The sample chamber was equipped with two, 0.05-mm thick windows covered with heat-resistant, X-ray transparent film comsisting of polytetrafluoroethylene.

Measurements

A θ-θ type X-ray diffractometer (Rint-Ultima III, Rigaku Co., Ltd.; CuKα radiation), with a goniometer radius of 285 mm, was used. The device had a parallel beam optical system using multi-layer mirrors of W and Si sheet crystals, with an incident beam slit of 1.0 mm. This mirror served as a monochromator for the elimination of CuKβ. A parallel beam slit, 100 mm long, with a resolution of 0.114º was also used. The sample chamber
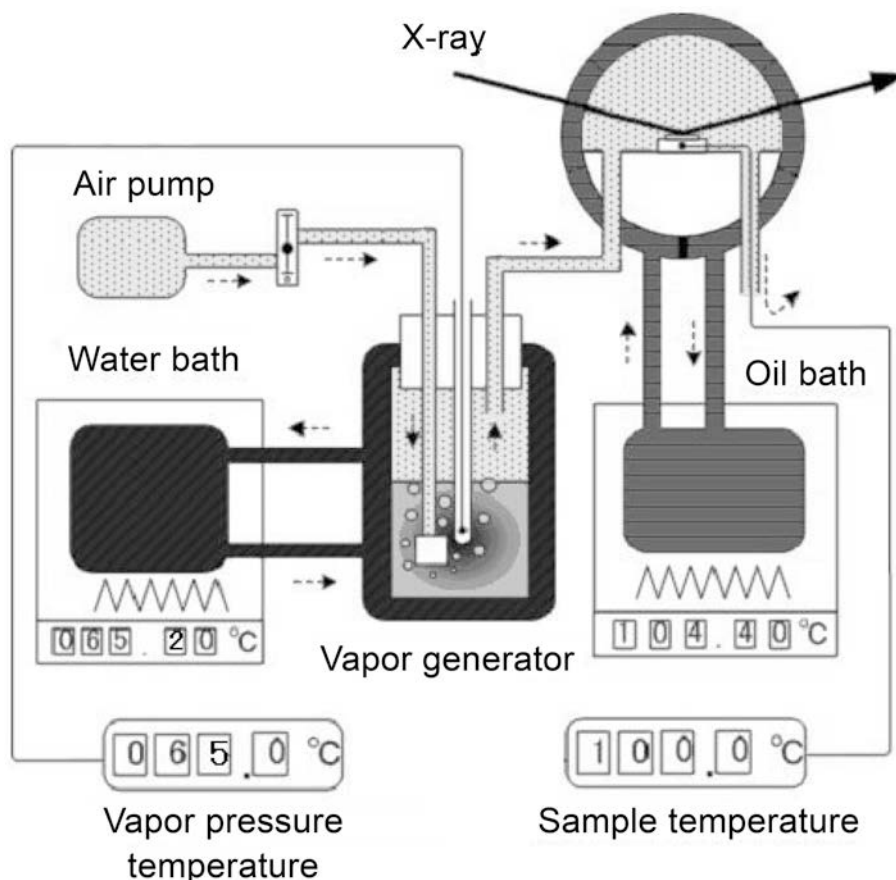

Figure 1. Schematic diagram of the sample environment-control system.

was set at the center of the goniometer. The measurement conditions were set such that the tube current was 30 mA, the voltage was 40 kV, and the scanning range was $2-12º2\theta$ for all temperature conditions. The scanning range of $2-32º2\theta$ was used for Na-montmorillonite at 50ºC and for Ca-montmorillonite at 70ºC to observe higher reflections. Beam overflow was absent at angles $>\sim2.9º2\theta$ for a parallel beam with a slit width of 1 mm and a sample length of 20 mm.

To consider the hysteresis effect, the sample was dried at a temperature of 10ºC greater than each sample temperature, and in extremely dry conditions (vapor-generator temperature = 6ºC) in the sample chamber before the measurements at each sample temperature. The sample temperature was set at 50, 70, 90, 110, 130, and 150ºC. The vapor pressure applied to the sample was from $P(H_2O) = 0.93$ kPa (the vapor-generator temperature = 6ºC) to just below the saturated condition at a sample temperature of <100ºC, or to $P(H_2O) = 81.47$ kPa (94ºC) at sample temperatures >100ºC. Repeated environmental *in situ* XRD measurements were performed for each increasing level of vapor pressure until the diffraction pattern showed no difference. Polarization, absorption, and base-line corrections were made for the 001 peak in order to obtain the basal spacing, which was measured at the 001 peak-top by interpolation. Unmodified diffraction data were used in all the figures.

RESULTS AND DISCUSSIONS

Na-montmorillonite

The XRD patterns (Table 1) for Na-montmorillonite for $2-32º2\theta$ at 50ºC (Figure 2), the 001 peaks at 70, 90, 110, 130, and 150ºC (Figures 3a−e), and plots of all d_{001} and corresponding FWHM values *vs.* RH (Figure 4a,b) led to the following observations.

Table 1. Temperature and RH conditions for XRD measurements.

Temperature (ºC)	RH (%) (vapor-generator temperature, ºC, $P(H_2O)$, kPa)	
	minimum	maximum
Na-montmorillonite		
50	7.6 (6, 0.93)	95.1 (49, 11.75)
70	3.0 (6, 0.93)	95.8 (69, 29.86)
90	3.3 (20, 2.34)	96.3 (89, 67.50)
110	1.6 (20, 2.34)	56.9 (94, 81.47)
130	0.3 (6, 0.93)	30.2 (94, 81.47)
150	0.3 (10, 1.23)	17.1 (94, 81.47)
Ca-montmorillonite		
50	7.6 (6, 0.93)	95.1 (49, 11.75)
70	3.0 (6, 0.93)	95.8 (69, 29.86)
90	1.3 (6, 0.93)	96.3 (89, 67.50)
110	0.7 (6, 0.93)	56.9 (94, 81.47)
130	0.3 (6, 0.93)	30.2 (94, 81.47)
150	0.2 (6, 0.93)	17.1 (94, 81.47)

001 peak profiles at 50ºC. At 50ºC, the basal spacings showed almost no change, *i.e.* $d_{001} = 9.9$ Å from RH = 7.6 to 21.4%, which is designated as the zero-layer hydration state (Figures 2, 4a). Under such conditions, the maximum peak intensity decreased gradually (Figure 2), and the FWHM increased from 0.9 to 1.4 Å with increasing RH (Figure 4b). The basal spacing increased abruptly from 9.9 Å (RH = 21.4%) to 12.0 Å (38.5%) (Figure 4a), which is designated as the trans-
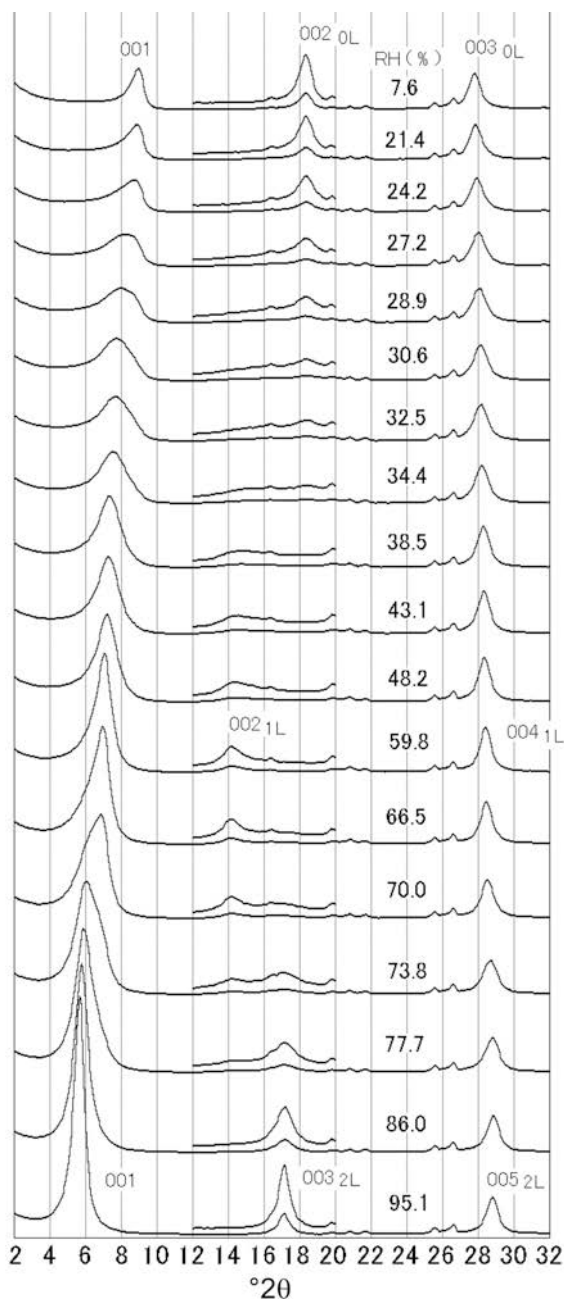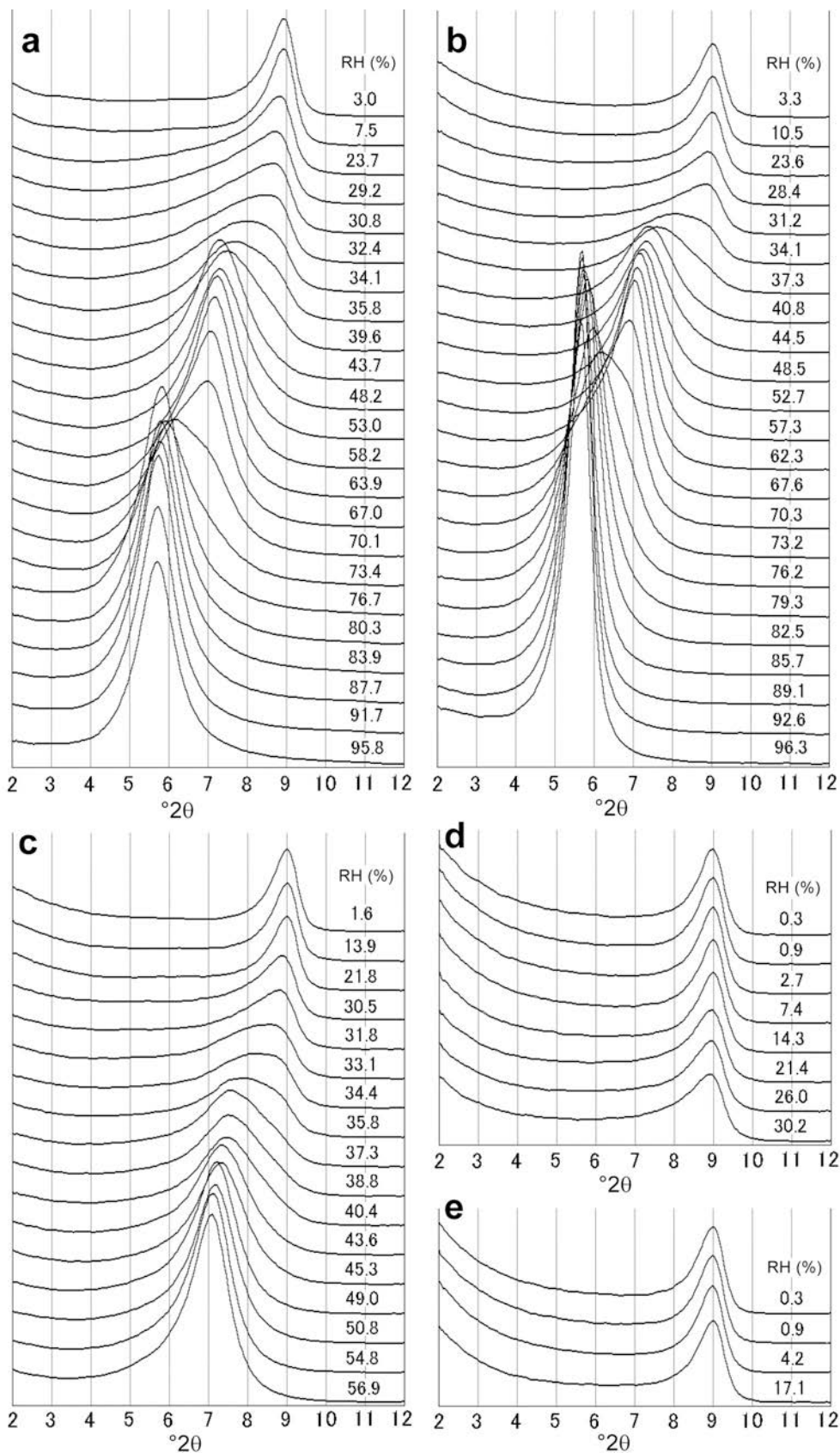

Figure 2. XRD profiles of Na-montmorillonite from $2-32º2\theta$ at 50ºC under various RH conditions. The intensity of the region between 12 and $20º2\theta$ is enlarged.
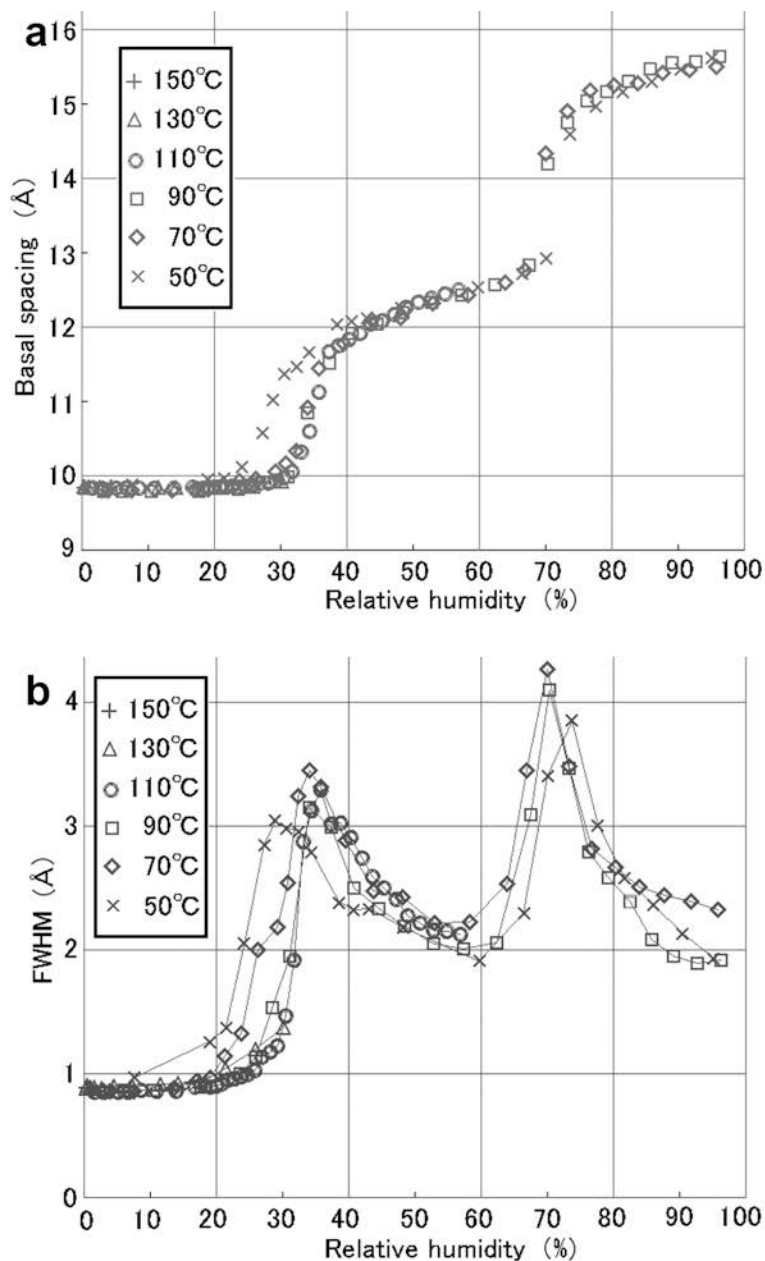
Figure 4. (a) Changes in the basal spacing of Na-montmorillonite with RH from 50 to 150ºC; (b) changes of the FWHM in Na-montmorillonite with RH from 50 to 150ºC.

formation region from the zero- to the one-molecular layer hydration state. In this transition state, single broad peaks were observed (Figure 2). The FWHM showed a maximum (3.0 Å) at RH = 28.9%, and decreased from 3.0 Å (28.9%) to 1.9 Å (59.8%) (Figure 4b). The maximum peak intensity showed a minimum at RH = 27.2%, and increased from RH = 27.2 to 59.8%

(Figure 2). The basal spacing showed a small change, *i.e.* d_{001} = 12.0 Å (RH = 38.5%) to 12.9 Å (70.0%), which is designated as the one-layer hydration state. The one-molecular layer hydration state was predominant at RH = 59.8%, where the FWHM was the smallest and the peak maximum intensity was maximum. The basal spacing jumped from 12.9 Å (RH = 70.0%) to 14.6 Å

Figure 3 (*facing page*). (a) XRD profiles of Na-montmorillonite from $2-12º2\theta$ under various RH conditions and at 70ºC; (b) at 90ºC; (c) at 110ºC; (d) at 130ºC; and (e) at 150ºC.

(73.8%), which is designated as the transformation region from the one- to two-layer hydration state. The FWHM showed a maximum (3.8 Å), and the maximum intensity showed a second minimum for RH = 73.8%. In this transformation region, these peaks were definitely asymmetric. At least two different domains of mixed-layer stacking are suggested. The basal spacings of 15.0 Å (RH = 77.7%) to 15.6 Å (95.1%) are designated as corresponding to the two-layer hydration state. Under such conditions, the peak maximum intensity increased and the FWHM decreased. The two-layer hydration state was most predominant at the nearly saturated condition (RH = 95.1%). The three-layer hydration state was not observed in this RH range.

001 peak profiles at 70−150ºC. The changes in diffraction profiles for sample temperatures of 70 and 90ºC (Figure 3a,b) *vs.* RH were almost the same as those at 50ºC (Figure 2). The basal spacing increased from the zero- (RH = 1.6%) to one-layer hydration state (56.9%) at 110ºC (Figure 3c), and the change was almost the same at 50ºC in this RH range. The basal spacing showed a small change for these experimental conditions at 130ºC (Figure 3d); however, the FWHM increased gradually and the maximum peak intensity decreased with increasing RH. No change was observed in the diffraction patterns from RH = 0.03 to 17.1% at 150ºC (Figure 3e). The three-layer hydration state was not observed for any sample temperatures.

The comparison against temperature. The swelling behavior of Na-montmorillonite *vs.* RH was almost identical for various temperatures (Figure 4a,b). The swelling curves between the zero- and one-layer hydration states moved systematically to greater RH and gradually approached that at the sample temperature of 110ºC (Figure 4a). The changes in the swelling behavior between the one- and two-layer hydration states for 50, 70, and 90ºC were observed at almost the same RH condition (~70%) (Figure 4a).

Wide-angle pattern at 50ºC. At 50ºC, the peak at ~18.3º2θ was observed under extremely dry conditions (RH = 7.6%), as shown in Figure 2 (with the peak enlarged for better illustration). The *d* value for this peak was ~4.8 Å, which is approximately half of the unhydrated basal spacing. This peak is assigned to the 002 peak and hereafter denoted as 002_{0L}. The 002_{1L} peak at ~14.2º2θ was observed in the one-layer hydration state (RH = 59.8%). The 003_{2L} peak at ~17.2º2θ was observed at the two-layer hydration state (RH = 95.1%). The maximum peak intensity of 002_{0L} was greatest at the zero-layer hydration state. The maximum peak intensity of 002_{0L} decreased and that of 002_{1L} increased gradually with increasing RH; however, both peak positions showed almost no change. The maximum peak intensity of 002_{1L} was greatest at

the one-layer hydration state. The maximum peak intensity of 002_{1L} decreased and that of 003_{2L} increased gradually with increasing RH; however, these two peak positions also showed almost no change. The maximum peak intensity of 003_{2L} was greatest at the two-layer hydration state.

The 003_{0L} peak at ~27.7º2θ was observed under extremely dry conditions (Figure 2). The peak position moved continuously toward greater angles with increasing RH. The peak at ~28.4º2θ was observed in the one-layer hydration state and is consistent with 004_{1L}. The peak at 28.8º2θ was observed in the two-layer hydration state and is consistent with 005_{2L}. During the zero-layer, one-layer, and two-layer development, the 003_{0L} and 004_{1L} peaks overlap. The same was observed for 004_{1L} and 005_{2L}. Peaks for 003_{1L}, 002_{2L}, and 004_{2L} were not observed.

The peaks at 20.9º2θ and 26.7º2θ belong to quartz. The peaks at 19.9º2θ, 21.8º2θ, and 25.8º2θ were weak and did not change with RH.

Ca-montmorillonite

The XRD patterns for Ca-montmorillonite over the range 2−32º2θ at 70ºC (Figure 5); the 001 peaks at 70, 90, 110, 130, and 150ºC (Figures 6a−e); and plots of all d_{001} and the corresponding FWHM values *vs.* RH (Figures 7a,b) provided the basis for the following.

001 peak profiles at 70ºC. At 70ºC, the basal spacing and the FWHM were 12.0 and 1.4 Å, respectively, under extremely dry conditions (RH = 3.0%) (Figures 5, 7a,b). The basal spacing increased continuously from 12.0 Å (RH = 3.0%) to 15.8 Å (95.8%) (Figure 7a). The FWHM increased from 1.4 Å (RH = 3.0) to 3.1 Å (21.3%) (Figure 7b). Under these conditions, the maximum peak intensity decreased continuously (Figure 5). At RH ≈ 20%, the swelling curve was steepest (Figure 7a) and the FWHM was maximum at 3.1 Å (Figure 7b), which is designated as the transformation region from the one- to two-layer hydration state. In this transition state, these peaks were symmetric (Figure 5) and FWHM values (Figure 7b) were small compared with Na-montmorillonite (Figures 2, 4b). The FWHM decreased from 3.1 Å (RH = 21.3%) to 1.9 Å (39.6%) (Figure 7b). Under such conditions, the maximum peak intensity increased continuously (Figure 5). The basal spacing increased gradually from 15.0 Å (RH = 39.8%) to 15.8 Å (95.8%), which is designated as the two-layer hydration state. Under such conditions, the FWHM was almost constant at ~1.9 Å and the maximum peak intensity was almost unchanged. The three-layer hydration state was not observed in this RH range.

001 peak profiles at 50ºC and 90−150ºC. The basal spacing increased continuously with increasing RH from 12.7, 11.8, and 11.0 Å up to the designated two-layer hydration state at 50, 90, and 110ºC, respectively (Figure 6a−c). At 130ºC, the basal spacing increased
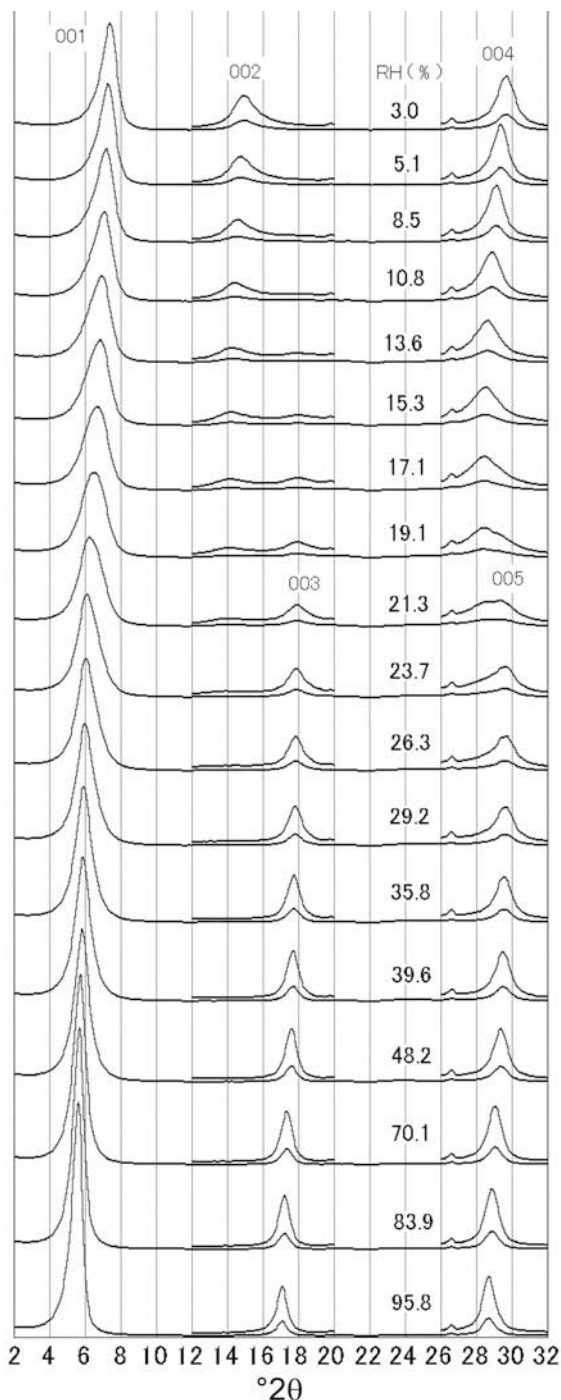
Figure 5. XRD profiles of Ca-montmorillonite from $2-32º2\theta$ under various RH conditions, at 70ºC. The intensity of the regions between 12 and $20º2\theta$ and 26 and $32º2\theta$ is enlarged.

from 10.2 Å (RH = 0.3%) to 14.6 Å (30.2%) (Figure 6d). At 150ºC, the basal spacing corresponded to the zero-layer hydration state from RH = 0.2 to 5.0%, and increased to 12.2 Å (RH = 17.1%) (Figure 6e). The three-layer hydration state was not observed at any sample temperature in this RH range.

The comparison against temperature. For various temperatures, the swelling behavior of Ca-mont-morillonite with RH differed at low RH conditions, where the d_{001} value decreased with increasing tempera-ture (Figure 7a). The greater the temperature the more zero-layers are designated to be present under extremely dry conditions. The swelling curves did not show a plateau for the one-layer hydration state for any sample temperature (Figure 7a), which is different from Na-montmorillonite (Figure 4a). The swelling curves moved gradually to greater RH with temperature (Figure 7a) which is similar to the transformation region between the zero- and one-layer hydration states in Na-mont-morillonite (Figure 4a). At 130 and 150ºC, the FWHM showed a bulge for the transformation region (RH $\approx$ 7%) from the zero- to one-layer hydration state (Figure 7b); however, this bulge was small and the FWHM at the position of the typical one-layer hydration state ($d_{001} \approx 12.0-12.5$ Å) remained relatively large, which is different from Na-montmorillonite. The swel-ling curves were steepest ($d_{001} \approx 13.5$ Å) (Figure 7a), and the FWHM showed a maximum at $3.0-3.6$ Å at RH $\approx$ 20%, which is the transformation region from the one- to two-layer hydration state (Figure 7b). The maximum of FWHM for RH $\approx$ 20% increased from 3.0 Å (50ºC) to 3.6 Å (130ºC) with increasing temperature.

Wide-angle pattern at 70ºC. At 70ºC, the 002 (14.8º2θ) and 004 peaks (29.7º2θ) were observed from RH = 3.0 to ~19.1% (Figure 5). These peak positions moved con-tinuously to the lower-angle side, and the maximum peak intensity decreased gradually with increasing RH, which is different from Na-montmorillonite (Figure 2). The 003 (17.9º2θ) and 005 peaks (29.8º2θ) were observed from RH $\approx$ 17.1 and 21.3 to 95.8%, respectively (Figure 5). These peak positions also moved continuously to the lower-angle side, and the maximum peak intensity increased gradually with increasing RH.

The differences between Na- and Ca-montmorillonite

The swelling behavior of Na-montmorillonite showed clearly the zero-, one-, and two-layer hydration states and the two transition states for all sample temperatures. The Ca-montmorillonite did not have a definite one-layer hydration state, as revealed for the first time by the present high-temperature observation. These differences relate to the hydration energy of the exchangeable cations (Mooney *et al.* 1952).

CONCLUSIONS

For both Na- and Ca-montmorillonite, the swelling curves were almost the same as those in figure 3 of Watanabe and Sato (1988) and in figure 3 of Ferrage *et al.* (2005a). The d_{001} reflection of Ca-montmorillonite at
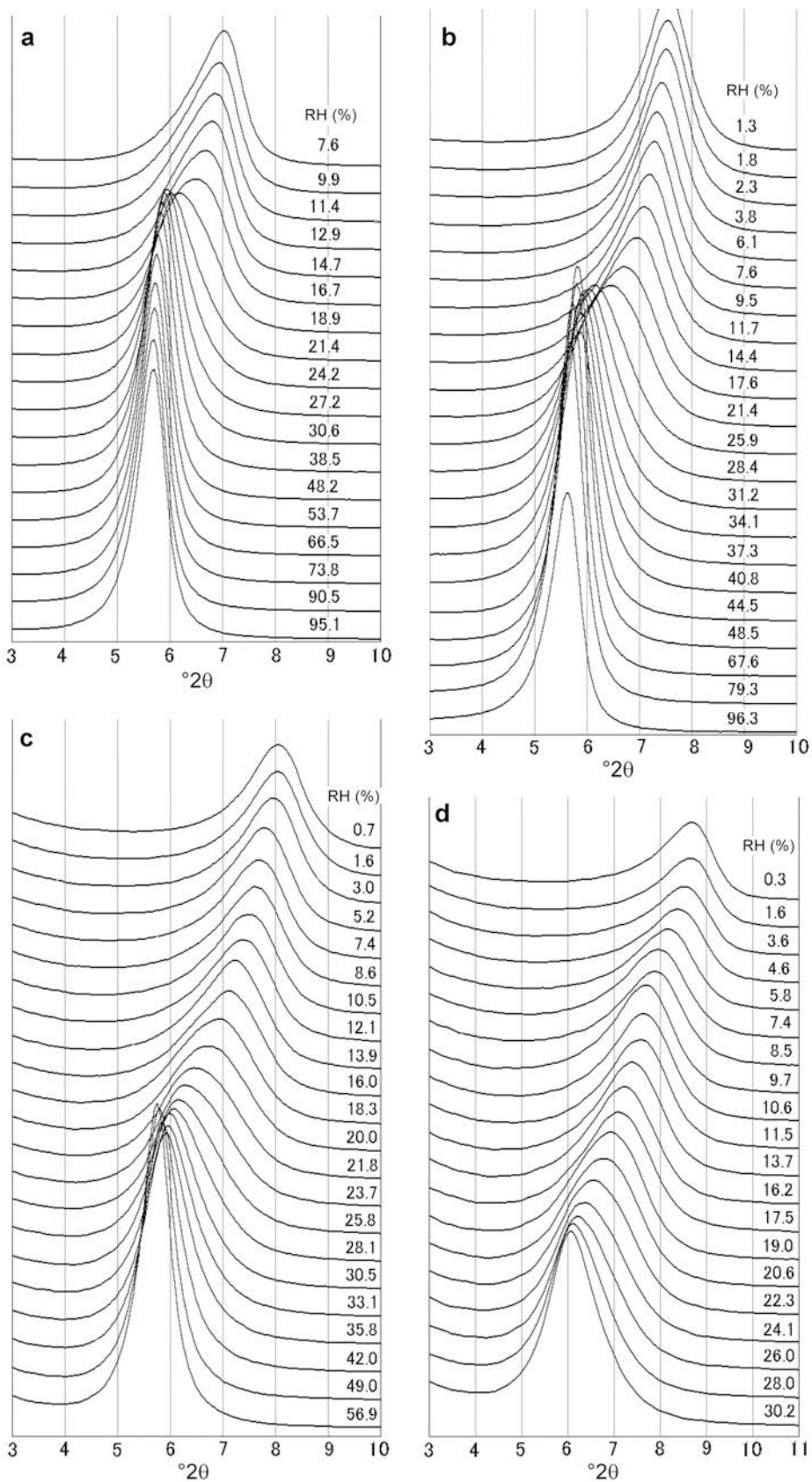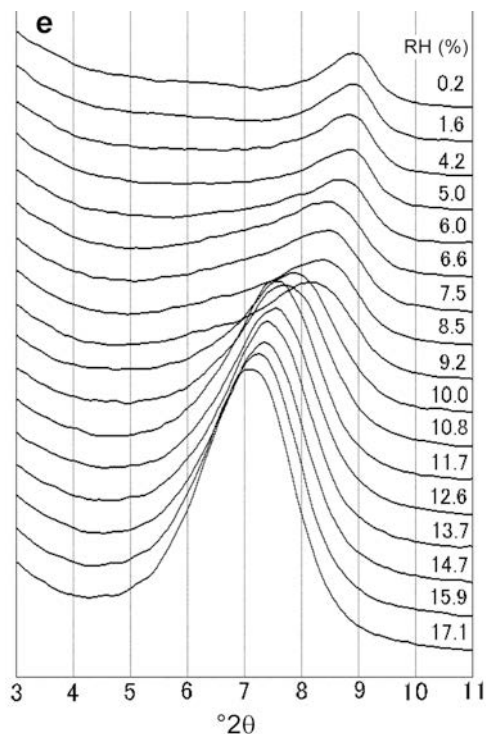
Figure 6 (*facing page and above*). (a) XRD profiles of Ca-montmorillonite from 2−12°2θ under various RH conditions and at 50°C; (b) at 90°C; (c) at 110°C; (d) at 130°C; and (e) at 150°C.
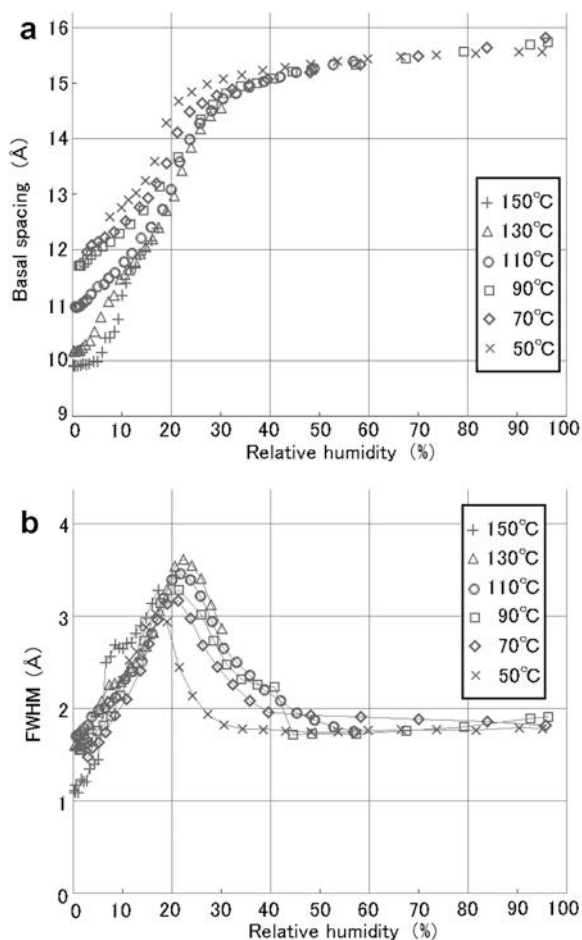

Figure 7. (a) Changes in the basal spacing of Ca-montmorillonite with RH from 50 to 150°C; (b) changes in the FWHM of Ca-montmorillonite with RH from 50 to 150°C.

high temperatures (reported here) is smaller than the values reported in those aforementioned works. In the present study, more detailed swelling curves were observed, especially at the transition regions. The three-layer hydration state was not observed in this study because the experimental RH region was from ~1 to 95% and the three-layer hydration state is observed only at RH ≈ 100% (figure 3 of Watanabe and Sato, 1988, and figure 2 of Moore and Hower, 1986).

Detailed discussion of the swelling behavior based on these experiments alone would be inappropriate. In order to understand the swelling behavior and the structure in detail, the swelling behavior of montmorillonite with a wider variety of cations (*i.e.* Li^+, Na^+, K^+, Rb^+, Cs^+, Mg^{2+}, Ca^{2+}, Sr^{2+}, Ba^{2+}, and La^{3+}) and at various temperatures will be examined in a future study. X-ray diffraction-pattern simulations, in which patterns are calculated by the stacking sequence of some one-dimensional clay unit models, will also be performed in a future study.

ACKNOWLEDGMENTS

REFERENCES

Ben Brahim, J., Armagan, N., Besson, G., and Tchoubar, C. (1983) X-ray diffraction studies on the arrangement of water molecules in a smectite. I. Homogeneous two-water-layer Na-beidellite. *Journal of Applied Crystallography*, **16**, 264−269.

Bradley, W.F., Grim, R.E., and Clark, G.F. (1937) A study of the behavior of montmorillonite upon wetting. *Zeitschrift für Kristallographie*, **97**, 216−222.

Ferrage, E., Lanson, B., Sakharov, B.A., and Drits, V. A. (2005a) Investigation of smectite hydration properties by modeling experimental X-ray diffraction patterns. Part I. Montmorillonite hydration properties. *American Mineralogist*, **90**, 1358−1374.

Ferrage, E., Lanson, B., Malikova, N., Plançon, A., Sakharov, B.A., and Drits, V.A. (2005b) New insights on the distribution of interlayer water in bi-hydrated smectite from X-ray diffraction profile modeling of 00*l* reflections. *Chemistry of Materials*, **17**, 3499−3512.

Ferrage, E., Lanson, B., Sakharov, B.A., Geoffroy, N., Jacquot, E., and Drits, V.A. (2007) Investigation of dioctahedral smectite hydration properties by modeling of X-ray diffraction profiles: Influence of layer charge and charge location. *American Mineralogist*, **92**, 1731−1743.

Hendricks, S.B., Nelson, R.A., and Alexander, L.T. (1940)

Hydration mechanism of the clay mineral montmorillonite saturated with various cations. *Journal of the American Chemical Society*, **62**, 1457−1464.

Ito, M., Okamoto, M., Shibata, M., Sasaki, Y., Danbara, T., Suzuki, K., and Watanabe, T. (1993) *Mineral composition analysis of bentonite*. PNC TN8430 93-003, Japan Atomic Energy Agency (in Japanese).

Iwasaki, T. and Watanabe, T. (1988) Distribution of Ca and Na ions in dioctahedral smectites and interstratified dioctahedral mica/smectites. *Clays and Clay Minerals*, **36**, 73−82.

Kakinoki, J. and Komura, Y. (1952) Intensity of X-ray diffraction by one-dimensionally disordered crystals. I. General derivation in cases of the 'Reichweite' S=0 and 1. *Journal of Physical Society of Japan*, **7**, 30−35.

Kawamura, K., Ichikawa, Y., Nakano, M., Kitayama, K., and Kawamura, H. (1999) Swelling properties of smectite up to 90ºC: In situ X-ray diffraction experimental and molecular dynamics simulation. *Engineering Geology*, **54**, 75−79.

MacEwan, D.M.C. (1958) Fourier transform methods for studying X-ray scattering from lamellar systems. II. The calculation of X-ray diffraction effects for various types of interstratification. *Kolloidzeitschrift*, **156**, 61−67.

Mooney, R.W., Keenan, A.G., and Wood, L.A. (1952) Adsorption of water vapor by montmorillonite. II. Effect of exchangeable ions and lattice swelling as measured by X-ray diffraction. *Journal of the American Chemical Society*, **74**, 1371−1374.

Moore, D.M. and Hower, J. (1986) Ordered interstratification of dehydrated and hydrated Na-smectite. *Clays and Clay Minerals*, **34**, 379−384.

Nagelschmidt, G. (1936) On the lattice shrinkage and structure of montmorillonite. *Zeitschrift für Kristallographie*, **93**, 481−487.

Nakazawa, H., Yamada, H., and Fujita, T. (1992) Crystal synthesis of smectite applying very high pressure and temperature. *Applied Clay Science*, **6**, 395−401.

Prost, R. (1975) Étude de l'hydratation des argiles: Interactions eau-minéral et mécanisme de la rétention de l'eau. II. − Étude d'une smectite (hectorite). *Annales Agronomique*, **26**, 463−535.

Reynolds, R.C. and Hower, J. (1970) The nature of interlayering in mixed-layer illite-montmorillonites. *Clays and Clay Minerals*, **18**, 25−36.

Sato, T., Watanabe, T., and Otsuka, R. (1992) Effects of layer charge, charge location, and energy change on expansion properties of dioctahedral smectites. *Clays and Clay Minerals*, **40**, 103−113.

Suquet, H., De La Calle, C., and Pezerat, H. (1975) Swelling and structural organization of saponite. *Clays and Clay Minerals*, **34**, 379−384.

Tamura, K., Yamada, H., and Nakazawa, H. (2000) Stepwise hydration of high-quality synthetic smectite with various cations. *Clays and Clay Minerals*, **48**, 400−404.

Watanabe, T. (1988) The structural model of illite/smectite interstratified mineral and the diagram for its identification. *Clay Science*, **7**, 97−114.

Watanabe, T. and Sato, T. (1988) Expansion characteristics of montmorillonite and saponite under various relative humidity conditions. *Clay Science*, **7**, 129−138.

Yamada, H., Nakazawa, H., Hashizume, H., Shimomura, S., and Watanabe, T. (1994) Hydration behavior of Na-smectite crystals synthesized at high pressure and high temperature. *Clays and Clay Minerals*, **42**, 77−80.